




Cite this: *RSC Adv.*, 2019, 9, 16271

## Fabrication of a novel high-performance leather waste-based composite retention aid

Yaohui You, \* Jiayong Zhang and Xubing Sun\*

In this study, a novel biomass composite retention aid was developed by using collagen hydrolysate (CH) extracted from collagen waste as the starting material, glutaraldehyde as the organic crosslinking agent and polymeric aluminum chloride (PAC) as the inorganic modifying agent. The as-prepared retention aids were characterized by gel chromatography, hydrodynamic diameter, zeta potential, transmission electron microscope (TEM), ultraviolet-visible adsorption spectra (UV-Vis), Fourier infrared spectrometer (FT-IR), and X-ray photoelectron spectroscopy (XPS). The results indicated that glutaraldehyde increased the molecular size of CH (*i.e.*, CCH) through the crosslinking reaction between the aldehyde group of glutaraldehyde and the primary amine group of CH. Subsequently, the PAC further increased cationic charge density and molecular size of CCH (*i.e.*, PAC-CCH) by the coordination interaction and self-assembly, thereby endowing PAC-CCH with better charge neutralization and bridging flocculation abilities. Compared to CH, CCH and PAC, the PAC-CCH exhibited excellent retention and drainage performances, and the best retention rate was greater than 85% at the dosage of 0.6 wt%. Our experimental results suggest that collagen wastes have a great potential to produce novel high-performance retention aids.

Received 31st March 2019

Accepted 20th May 2019

DOI: 10.1039/c9ra02407g

[rsc.li/rsc-advances](http://rsc.li/rsc-advances)

## Introduction

In the process of papermaking, retention aids are usually introduced into the stock suspension to improve the performance of retention and dewatering during sheet formation, which play an essential role of the aggregation of fillers and fiber fines through charge neutralization/patch and bridging flocculation.<sup>1–4</sup> Considering higher filler filling and higher speed paper machine, retention aids have become particularly important.

Typical retention aids are single- or multicomponent, and microparticle systems involving synthetic or natural polymers.<sup>5–10</sup> Synthetic polymers, such as polyacrylamide derivatives, exhibit satisfactory retention performance at a low dosage, but they are nonrenewable resources and have harmful effects on the environment.<sup>11,12</sup> Among natural polymers, starch derivatives have the advantages of being biodegradable and inexpensive; however, they usually require a relatively high dosage to obtain a desired retention performance.<sup>6</sup> Chitosan and guar gum derivatives are only used in high-grade and specialty paper, or stay in the laboratory stage due to their high-cost and/or complicated process technology.<sup>7,13</sup> In recent years, the utilization of low cost biomass, including cassava dreg, microfibrillated cellulose, and tara gum,<sup>1,14</sup> has received

considerable attention. Unfortunately, these products are not satisfactory in view of their practicality, economy and operability. Hence, it is an important challenge to develop novel, low-cost, high-performance biomass-based retention aids with simple synthesis processes.

The tannery industry inevitably produces a great amount of collagen wastes due to the trimming, splitting and shaving operations. This collagen waste is a valuable biomass resource and could result in serious environmental problems if they are not properly disposed.<sup>15</sup> Collagen wastes can be hydrolyzed into collagen hydrolysate (CH) with molecular weights ranging from a few thousand to several hundred thousand Da.<sup>16</sup> It is well known that collagen hydrolysate is a kind of water-soluble polymer and has abundant amino, carbonyl, hydroxyl, and acylamino groups, which exhibit charge neutralization/patch and bridging flocculation ability to some extent.<sup>17</sup> In fact, the casein, the major protein in milk, was once used in papermaking to improve the surface strength and printing function of paper.<sup>18</sup> Furthermore, our previous study has demonstrated that increasing the molecular weight of gelatin using glutaraldehyde as a cross-linking agent could improve its flocculation ability.<sup>19</sup> These facts suggest that a novel retention aid could be prepared by using collagen wastes as raw material.

Further analysis indicated that the isoelectric points of CH and cross-linked collagen hydrolysate (prepared by glutaraldehyde as the cross-linking agent, denoted as CCH) are both below 5. Therefore, their charge neutralization/patch abilities with anionic fillers and fiber fines are very limited under neutral

Key Laboratory of Fruit Waste Treatment and Resource Recycling of the Sichuan Provincial Higher Learning Institutes, Neijiang, Sichuan Province 641100, China. E-mail: [allenyoyahui@163.com](mailto:allenyoyahui@163.com); [xbsnj123@sina.com](mailto:xbsnj123@sina.com)



condition.<sup>20</sup> On the other hand, even for CCH, the molecular weight is still much smaller (approximately  $5 \times 10^5$  Da) compared with that of polyacrylamide and starch (far higher than  $1 \times 10^6$  Da).<sup>21</sup> Hence, a further increase of cationic charge density and molecular weight of CCH may be a good choice for improving retention and drainage performance. Nevertheless, the conventional methods, such as quaternization, crosslinking or grafting reactions, usually occurring in the primary amine groups of CCH,<sup>22–25</sup> have shown difficulty in meeting the requirements for increasing both cationic charge density and molecular weight of CCH because of the limited number of primary amine groups. Therefore, a special chemical with high density of positive charge and interaction ability with CCH should be selected to modify CCH.

Polymeric aluminum chloride (PAC), a group of specific aluminum salts including monomeric aluminum, dimeric aluminum ( $\text{Al}_2$ ),  $\text{Al}_{13}\text{O}_4(\text{OH})_{24}(\text{H}_2\text{O})_{12}^{7+}$  ( $\text{Al}_{13}$  Keggin) and  $\text{Al}_{30}\text{O}_8(\text{OH})_{56}(\text{H}_2\text{O})_{24}^{18+}$  ( $\text{Al}_{30}$  Keggin), is positively charged under acidic and neutral conditions.<sup>26</sup> It has been demonstrated that the active species of PAC is mainly  $\text{Al}_{13}$  Keggin.<sup>27</sup> In papermaking, PAC has been used as a rosin size bonding agent, anionic trash catcher, retention aid and flocculant due to its high cationic charge density.<sup>28</sup> However, retention performance has shown difficulty in meeting the requirement when only PAC is used due to its limited bridging ability, and excess PAC easily cause electrolyte imbalance of the pulp.<sup>2</sup> More interestingly, aluminum salt has been used as a tanning or crosslinking agent in leather manufacturing because of its considerably strong coordination ability with polar groups of collagen,<sup>29,30</sup> which means that it can further increase the molecular weight of CCH if PAC was selected to modify CCH, thereby facilitating its bridging flocculation performance. Considering all advantages of PAC and CCH, it is reasonable to suggest that PAC and CCH can be used as an effective retention system to provide a new strategy for the development novel biomass based retention aids with excellent performance. However, to the best of our knowledge, no similar studies have been performed.

In the present work, CH was first prepared by pepsin hydrolysis collagen wastes, and CCH was prepared by glutaraldehyde cross-linked CH. Subsequently, the PAC–CCH composite retention aid was obtained by PAC-modified CCH. The characterizations of CH, CCH and PAC–CCH were investigated by gel chromatography, hydrodynamic diameter, zeta potential, transmission electron microscope (TEM), ultraviolet-visible adsorption spectra (UV-Vis), Fourier infrared spectrometer (FT-IR), and X-ray photoelectron spectroscopy (XPS). Finally, the performance and mechanism of as-prepared retention aids were systematic studied.

## Experimental

### Materials

Collagen waste supplied by a local tannery (Sichuan, CN) was generated from shaving pigskin wet-white, where the pigskin wet-white without chrome tanning was obtained by treating conventionally delimed pelts with sodium sulfate. Pepsin extracted from pig stomach (activity 220 000 U  $\text{g}^{-1}$  at 38 °C and

pH = 2) was purchased from Hongrunbaoshun Technology (Beijing, China). bleached bamboo kraft pulp (beating degree = 23 °SR) were obtained from Yongfeng Paper Mill (Sichuan, CN). Kaolin with 350 mesh as model filler was purchased from the Fengcheng Chemical Reagent Factory (Shanghai, CN). Polymeric aluminum chloride (PAC) was purchased from Gongyi Midea Water Purifying Material Co., Ltd. (Henan, CN), and the content of  $\text{Al}_2\text{O}_3$  was 30%. All other chemicals were all of analytical grade.

### Preparation of CH, CCH, and PAC–CCH

The collagen waste was fully washed to remove impurities and then dried at 60 °C for 12 h. Fifty g of the dry collagen waste was suspended in 500 mL of water and the pH of the suspension was adjusted to 2.0. Then 0.5 g of pepsin was added to the suspension and the reaction was performed at 38 °C for 3 h. Subsequently, the pH of the suspension was adjusted to 5.0, and the suspension was cooked at 100 °C for 5 min. Finally, the filtrate was collected, freeze-dried and smashed, after which the CH powder was obtained. The physiochemical properties of collagen waste and CH powder are shown in Table 1. As shown in Table 1, all the samples were free of aluminum and chrome, and sufficient washing could remove most impurities of the collagen waste, such as inorganic salts and particles.

CCH was prepared according to the procedures in our previous work.<sup>19</sup> In an optimal manner, 5 g of CH was dissolved in 100 mL of distilled water and the pH of the solution was adjusted to 7.0. Then 0.5 mL of 50% glutaraldehyde solution was added dropwise into CH solution and the reaction was performed at 40 °C for 3 h. The final CCH with crosslinking degree of 0.81 was obtained. PAC–CCH was prepared as follow: in an optimal manner, a defined amount of PAC solution was added dropwise into CCH solution, and the final PAC and CCH concentrations were fixed at 2.5  $\text{g L}^{-1}$  and 5  $\text{g L}^{-1}$ , respectively. Then, the mixture solution was stirred at 300 rpm for 20 min at room temperature. To eliminate the disturbance of unreacted glutaraldehyde or PAC, both CCH and PAC–CCH solutions were purified using a dialysis bag with a molecular weight cut-off 10 000 Da, and were then lyophilized and smashed.

### Characterization of retention aid

The average molecular weight of the sample was characterized by gel chromatography test (Viscotek 270max GPC/SEC,

Table 1 Physiochemical properties of collagen wastes and CH powder

	Collagen waste <sup>a</sup>	Collagen waste <sup>b</sup>	CH powder
Protein%	39.4	92.4	95.7
Ash%	10.1	2.6	1.7
Moisture%	47.2	3.8	1.6
Aluminum%	— <sup>c</sup>	— <sup>c</sup>	— <sup>c</sup>
Chrome%	— <sup>c</sup>	— <sup>c</sup>	— <sup>c</sup>

<sup>a</sup> Without washing and drying. <sup>b</sup> With washing and drying. <sup>c</sup> Not detected.



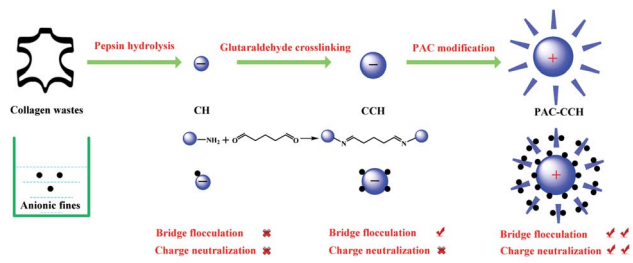


Fig. 1 Schematic illustration for the preparation of collagen wastes based retention aid.

Table 2 Average molecular weight, isoelectric point and hydrodynamic diameter of sample

Sample <sup>a</sup>	CH	CCH	PAC-CCH
Average molecular weight (kDa)	120	500	— <sup>b</sup>
Isoelectric point	4.8	4.5	7.5
Hydrodynamic diameter (nm)	85	280	3300

<sup>a</sup> The concentration of samples was 0.5 g L<sup>-1</sup>. <sup>b</sup> Not detected.

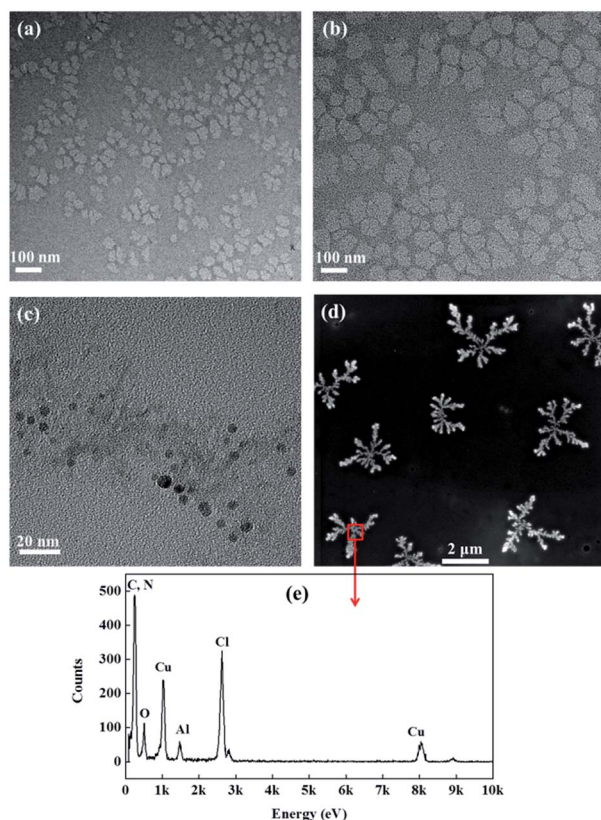


Fig. 2 TEM micrographs of (a) CH, (b) CCH, (c) PAC, (d) PAC-CCH, and (e) EDX analysis of PAC-CCH. The concentration of samples was 0.25 g L<sup>-1</sup>.

Malvern, UK). Hydrodynamic diameter, a parameter commonly used to characterize the size of the polymer chain in solution, was determined by a nanoparticle zeta instrument (Litesizer 500, Anton Paar, AT). The isoelectric points of samples were

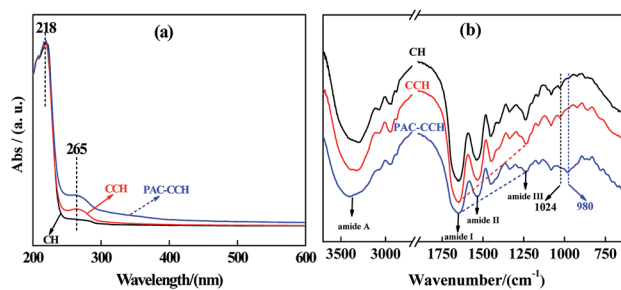


Fig. 3 (a) UV-Vis spectra of CH, CCH and PAC-CCH. The concentration of samples was 0.5 g L<sup>-1</sup>; (b) FT-IR spectra of CH, CCH and PAC-CCH.

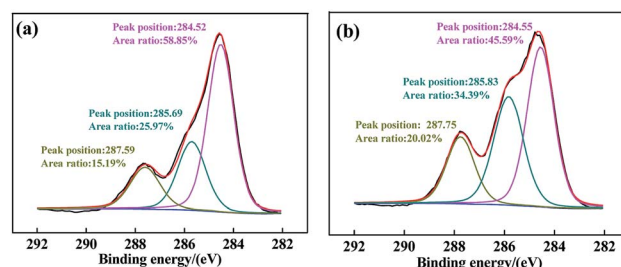


Fig. 4 C(1s) XPS spectra of (a) CCH and (b) PAC-CCH.

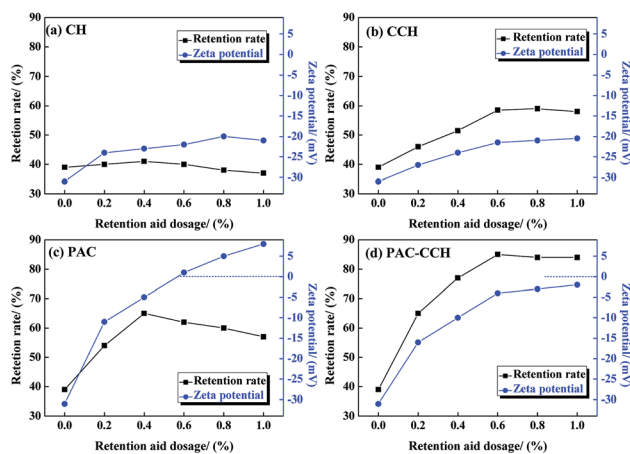


Fig. 5 Effects of retention aids with varying dosage on retention rate and zeta potential of pulp suspension: (a) CH, (b) CCH, (c) PAC, (d) PAC-CCH.

estimated by determining their zeta potentials using a nanoparticle zeta instrument (Litesizer 500, Anton Paar, AT). The morphologies were observed and imaged by Transmission Electron Microscope (TEM; Tecnai G2 F20 S-TWIN, FEI, US). In this test, suitable amounts of sample solutions were adsorbed onto the copper net, followed by infrared drying for 5 min prior to analysis. The ultraviolet-visible adsorption spectra of sample solutions were recorded by a spectrophotometer (UV-Vis; UV-2000, Shunyuheping, Shanghai, CN). Fourier infrared analyses were carried out by using compressed films of KBr and sample powders (FT-IR; Nicoletis10, Thermo Scientific, US). The



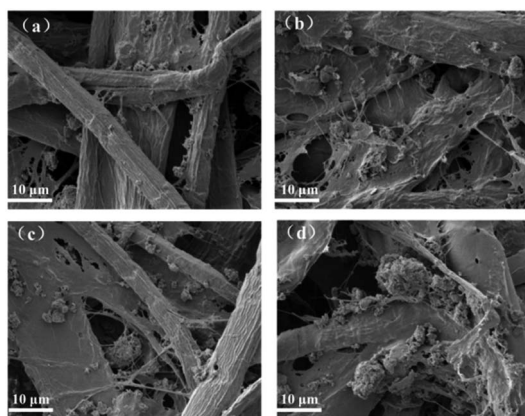


Fig. 6 FESEM micrographs of hand-sheet: (a) CH, (b) CCH, (c) PAC, (d) PAC-CCH.

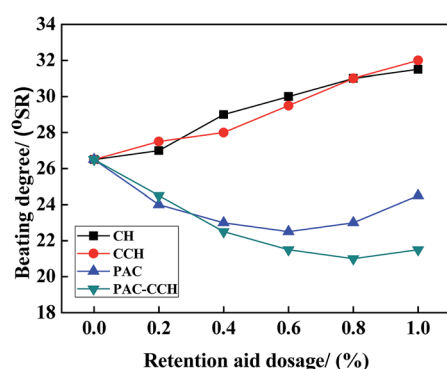


Fig. 7 Effect of different retention aids on the drainage performances.

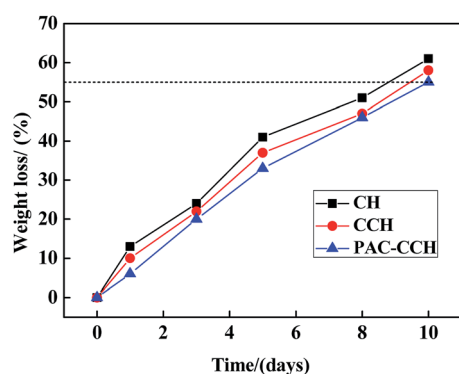


Fig. 8 Weight loss of different retention aids in soil burial.

surface element compositions and element chemical states of sample powders were analyzed by X-ray photoelectron spectroscopy (XPS; Kratos XSAM-800, UK) employing Mg-K $\alpha$  X-radiation ( $h\nu = 1253.6$  eV) and a pass energy of 31.5 eV. For XPS spectra, all of the binding energy peaks of spectra were calibrated by carbon C(1s) binding energy peak at 284.6 eV. Peaks from all the high resolution spectra were fitted with XPSPEAK 4.1 software using 20% Lorentzian-Gaussian.

## Retention and drainage performances test

The filler retention performances were conducted using a dynamic drainage jar with 100 mesh screen, which was designed by the author. 1 L pulp suspensions consisted of 5 g pulp and 1 g kaolin. The pH of pulp suspensions was adjusted to 7.0 and the stirrer speed was 250 rpm for the entire experimental procedure. A certain amount of retention aids (mass percentage relative to dry pulp) was added to pulp suspensions, and the filtrate was collected after 20 s and the wet hand-sheet was dried. The zeta potential of the pulp suspension was determined with a pulp zeta potential instrument (MütekSZP-10, BTG Instruments, SE). In this test, the mass concentration of pulp was 10 g L $^{-1}$ , and the other conditions were consistent with retention test. The morphology of fillers retained in the hand-sheets was observed and imaged by field emission scanning electron microscopy (FESEM; S-4800, Hitachi, Tokyo, JP). The samples were mounted on the base plate and coated with gold using vapor deposition techniques. The kaolin amount in the filtrate was tested by UV-Vis,<sup>31</sup> and the filler retention (%) was calculated as follows: filler retention (%) = (initial kaolin – kaolin of filtrate)/(initial kaolin).

The drainage performance was evaluated by Schopper-Riegler degree (°SR). The °SR was measured by using a YT-DJ-100 beating degree tester (Yante Science & Technology Co. Ltd., Jiangsu, CN), according to the China national standard ISO 5267-1 (1999). In this test, the mass concentration of pulp was 2 g L $^{-1}$ , and the other conditions were consistent with retention test.

## Biodegradation test

The biodegradability of the retention aid was evaluated by a soil burial test according to the literature.<sup>32</sup> Soil was taken from the surface layer of the ground near the Neijiang Normal University and was poured into a 500 mL beaker up to a thickness of approximately 8 cm. Before the soil burial test, 30 mL retention aid solutions with concentration of 5 g L $^{-1}$  were poured into a Teflon mould with a diameter 10 cm, and then dried at 40 °C for 24 h to obtain films. The as-prepared films were weighed and then buried in the soil to a depth of 3 cm at 25 °C. Water was sprayed twice a day to sustain the moisture. During the fixed periods (first, third, fifth, eighth and tenth day), the residual films were carefully taken out, washed, dried and weighed. The weight loss (%) was calculated and used as an index to appraise the biodegradability of retention aid.

## Results

### Preparation and characterization of retention aid

In this work, we sought to prepare a collagen waste based retention aid with excellent performance. However, as mentioned above, the retention performances of CH extracted from collagen wastes may be limited due to its poor charge neutralization/patch ability and low molecular weight. Therefore, glutaraldehyde was employed as an organic crosslinking agent to increase the molecular weight of CH (*i.e.*, CCH). Subsequently, PAC was chose as an inorganic modifying agent



to further improve charge neutralization ability and increase the molecular weight of CCH (*i.e.*, PAC-CCH). The preparation process of collagen waste based retention aid is shown in Fig. 1.

After glutaraldehyde crosslinking, the molecular weight of CCH (500 kDa) was almost four times higher than that of CH (120 kDa). Meanwhile, the isoelectric point of CCH (4.5) was slightly lower than that of CH (4.8), as shown in Table 2. These results were expected because the preparation of CCH was based on the crosslinking reaction between the aldehyde group of glutaraldehyde and the primary amine group of CH (as shown in Fig. 1), where the primary amine group can bind to a proton to become positively charged. Further modifying CCH by PAC, the isoelectric point of PAC-CCH (7.5) was significantly higher than that of CCH and CH, which directly indicated that PAC-CCH had a better charge neutralization ability than CCH and CH. Because the molecular size of PAC-CCH is so large and cannot pass through a 0.45  $\mu\text{m}$  filter membrane, its molecular weight cannot be directly quantified by gel chromatography. Here, the hydrodynamic diameter of CH, CCH and PAC-CCH solution was tested to indirectly evaluate the change of their molecular weights. It was found that PAC-CCH showed the highest hydrodynamic diameter, suggesting that PAC could further increase the molecular weight of CCH.

For visually observing changes in the molecular size and morphology, CH, CCH, PAC and PAC-CCH were characterized by TEM (Fig. 2). It is well-known that CH is a degradation product of collagen and its molecular size should be lower than that of collagen (collagen is 300 nm long and 1.5 nm in diameter). As shown in Fig. 2a, most CH curled into to an irregular accumulation body with a diameter of approximately 40 nm due to infrared drying. In contrast, the diameter of CCH was larger than that of CH (Fig. 2b) due to glutaraldehyde crosslinking. More remarkably, PAC-CCH formed an orderly, large, highly branched structure with a diameter above 2  $\mu\text{m}$  (Fig. 2d). These results coincided with that of the hydrodynamic diameter shown in Table 2. A similar phenomenon has also been reported by Wang *et al.*, where they found that polydimethyldiallylammonium chloride, a kind of synthetic polymer, could induce PAC to form a highly branch structure, maybe attributed to the interactions between them.<sup>33</sup> The energy dispersive X-ray (EDX) analysis (Fig. 2e) revealed that the complex observed in the TEM images had abundant aluminum and nitrogen elements (the characteristic elements of PAC and CCH, respectively), which directly confirmed that the complex was composed of PAC and CCH. According to the literature, as the active species of PAC, the size of a single  $\text{Al}_{13}$  particle is only a few nanometers, which is consistent with our observation results (Fig. 2c);  $\text{Al}_{13}$  is easy to self-assemble and forms chain-like cluster with a few hundred nanometers in aqueous solution.<sup>34</sup> Moreover, it has been reported that collagen peptides have the ability to self-assemble into large size collagen fibers under certain metal conditions.<sup>35,36</sup> Consequently, it is logical to reason that PAC-CCH forms a large-sized and highly branched complex due to the synergy of their strong interaction and self-assemble abilities.

The UV-visible spectra of CH, CCH and PAC-CCH are shown in Fig. 3a. It was obvious that all the samples displayed a strong

adsorption peak located approximately 218 nm, mainly ascribed to the  $\pi-\pi^*$  transition of the peptide chain's carbonyl.<sup>37</sup> Compared to CH, CCH showed a new adsorption peak at approximately 265 nm, which was ascribed to the  $n-\pi^*$  transition of the C=N group (*i.e.*, the formed Schiff base structure between the aldehyde group and primary amine group, as shown in Fig. 1).<sup>19</sup> This result also indicated that the crosslinking reaction between CH and glutaraldehyde was successfully performed. After modifying with PAC, the adsorption peak of PAC-CCH at approximately 265 nm was clearly higher than that of CCH. This was likely due to the fact that PAC combined with CCH to form a complex, leading to the extension of the CCH chain and further exposure of the C=N group.<sup>38,39</sup> However, the adsorption peak positions of PAC-CCH at approximately 218 nm and 265 nm were not significantly changed compared to those of CCH, indicating that the UV-visible spectra could not explicitly reveal the interaction sites between CCH and PAC.

Fig. 3b shows the FT-IR spectra of CH, CCH and PAC-CCH. The characteristic peaks approximately  $3300\text{ cm}^{-1}$ ,  $1640\text{ cm}^{-1}$ ,  $1540\text{ cm}^{-1}$  and  $1240\text{ cm}^{-1}$  respectively represented amide A (amide N-H stretching vibration), amide I (amide C=O stretching vibration), amide II (the coupling of N-H bending vibration and C-N stretching vibration) and amide III (the coupling of amide C-N stretching vibration and amide N-H in-plane bending vibration) of collagen.<sup>40</sup> Because the characteristic peak of C=N is located at approximately  $1620\text{ cm}^{-1}$ , which overlaps with that of the amide I, no new characteristic peak appeared in the FT-IR spectrum of CCH after glutaraldehyde crosslinking. For PAC-CCH, the characteristic peak of amide A was obviously broadened, which could be attributed to the formed hydrogen bond between PAC and CCH. Moreover, the relative intensity of the collagen characteristic peak (amide I, amide II and amide III) was changed, as indicated by the oblique lines in Fig. 3b, which implied that some sites of the collagen amide group was involved in the interaction between PAC and CCH.<sup>41</sup> In addition, the characteristic peak at approximately  $1024\text{ cm}^{-1}$  (the C-O stretching vibration) disappeared and a broad characteristic peak started to appear at approximately  $980\text{ cm}^{-1}$ , presumably corresponding to the coupling of C-O stretching vibration and Al-OH-Al stretching vibration.<sup>42,43</sup> All these observations provided evidence of the combinations between PAC and CCH.

To further explore the interaction mechanism between PAC and CCH, the high-resolution C(1s) spectra of CCH and PAC-CCH by XPS analysis were shown in Fig. 4. For CCH (Fig. 4a), the C(1s) spectrum was curve-fitted into three peaks at the binding energy of 284.52 eV (C-C/C-H), 285.69 eV (C-O/C-N), and 287.59 eV (N-C=O).<sup>44</sup> After modifying CCH with PAC (Fig. 4b), the relative peak areas of C-O/C-N and N-C=O in PAC-CCH were obviously higher than those of CCH, which suggested that an interaction between CCH and PAC led to the exposure of C-O/C-N and N-C=O in the surface of PAC-CCH. Moreover, compared to CCH, the peak position of C-O/C-N and N-C=O in PAC-CCH shifted to a higher binding energy (285.83 eV and 287.75 eV, respectively), indicating a decrease in electronic cloud density around the C atom, probably due to the electron



donating-accepting interaction (*i.e.*, coordination interaction) from C–O/C–N and N–C=O of CCH to aluminum ion of PAC.<sup>45,46</sup>

### The retention performance

Prior to preparing the PAC–CCH composite retention aid, the retention performance of only adding CH, CCH and PAC with varying dosages was investigated and the results are shown in Fig. 5a–c. It was found that CH was almost completely ineffective on retention performance, which was expected because of its low molecular weight and poor charge neutralization ability. In contrast, CCH showed a positive effect on retention performance, where the retention rate increased from 39% to 58% with the CCH dosage ranging from 0 to 0.6 wt%, after which it tended to be stable when the CCH dosage exceeded 0.6 wt%. The zeta potential results from Fig. 5b revealed that the zeta potential of the pulp suspension slightly improved after adding CCH, but was still way below zero for the whole dosage range, which indicated that the retention mechanism of CCH mainly depended on bridge flocculation due to the increased molecular weight. When only adding PAC, the retention rate increased from 39% to 65% with the PAC dosage ranging from 0 to 0.4 wt%, after which it was rapidly decreased when the PAC dosage exceeded 0.4 wt%. This result was attributed to the fact that appropriate PAC could induce aggregation of filler particles mainly through charge neutralization, whereas excess PAC could lead to charge reversal of pulp suspension and play a role in dispersion (the zeta potential results from Fig. 5c).<sup>47–49</sup> When PAC–CCH was added to the pulp suspension, the retention rate was clearly higher than that of CCH and PAC used alone, where the maximum retention rate reached 85% at a dosage of 0.6 wt% (Fig. 5d). Meanwhile, within the scope of this test dosage, PAC–CCH did not result in charge reversal of pulp suspension and had a widely effective dosage range. These results could be explained that PAC–CCH had both a higher molecular weight and desirable charge neutralization ability compared with CCH and PAC.

For directly observing the retention performance and floc size, the morphology of the hand-sheet by adding CH, CCH, PAC and PAC–CCH with the optimum dosage is shown in Fig. 6. It can be found that few small flocs adhered to the surface of fibers when CH was added (Fig. 6a). In contrast, the addition of CCH and PAC resulted in an increase in both the size and quantity of flocs (Fig. 6b and c). The most significant increase in both size and quantity of flocs could be observed when PAC–CCH was added (Fig. 6d), which directly confirmed that PAC–CCH had better retention performance than CH, CCH and PAC.

### The drainage performance

The drainage performance of pulp suspension has a great influence on the operation speed of the paper machine and the energy consumption of the paper drying. Schopper-Riegler degree ( $^{\circ}\text{SR}$ ) is an important parameter to evaluate the drainage performance of pulp suspension, where a lower  $^{\circ}\text{SR}$  represents better drainage performance. The  $^{\circ}\text{SR}$  values of pulp suspension with different dosage of CH, CCH, PAC and PAC–CCH are shown in Fig. 7. It was found that the drainage

performance of pulp suspension by adding CH or CCH gradually worsened with increasing dosage. This was probably because both CH and CCH blocked the pores of fiber and floc, reducing the amount of drained water due to their excellent hydrophilicity and film-forming property. When adding PAC, the drainage performance of pulp suspension first increased and then decreased with increasing dosage. In contrast, PAC–CCH showed the best drainage performance. This result could be explained as follows. First, PAC–CCH with good retention performance could induce fines to form larger-sized flocs (as seen in Fig. 6), leading to a significant decrease in solution viscosity and floc specific surface area, thereby greatly reducing the fluid flow resistance.<sup>9</sup> Second, PAC–CCH reduced the hydration of flocs and fibers due to its outstanding charge neutralization ability.<sup>50–52</sup> Therefore, good drainage performance of PAC–CCH can be expected.

### The biodegradation performance

The time dependence of weight losses of different retention aids in soil burial is shown in Fig. 8. It could be found that CH was the most sensitive material to the biodegrading medium, while PAC–CCH was the most resistant to microbial attack, which was attributed to the improvement of stability due to the cross-linking and coordination reaction.<sup>53</sup> However, beyond the eighth day, the weight losses of all the sample films were above 55%, and the residual films were not easily collected due to destruction of integrity. Therefore, from a practical point of view, all the retention aids might be classified as rapidly biodegradable materials.

## Conclusions

In summary, a novel biomass composite retention aid was facilely prepared using collagen hydrolysate extracted from collagen waste as the raw material. The as-prepared retention aid exhibited excellent retention and drainage performances because the bridging flocculation and charge neutralization abilities of collagen hydrolysate were greatly improved after glutaraldehyde crosslinking and PAC modification. Our research results suggest that the collagen hydrolysate extracted from collagen waste has a great potential to produce novel high-performance biomass-based retention aids.

## Conflicts of interest

There are no conflicts of interest to declare.

## Acknowledgements

This work was financially supported by the National Natural Science Foundation of China (No. 21506103), the Science and Technology Support Program of Sichuan Province (No. 2015GZ0170, 2019YJ0399), and the Major Training Program of the Education Department of Sichuan Province (No. 15CZ0026).



## References

- 1 M. Diab, D. Curtil, N. El-shinnawy, M. L. Hassan, I. F. Zeid and E. Mauret, *In. Crop. Prod.*, 2015, **72**, 34–45.
- 2 M. A. Hubbe, H. Nanko and M. R. Mcneal, *BioResources*, 2009, **4**, 850–906.
- 3 N. Cezar and H. N. Xiao, *Ind. Eng. Chem. Res.*, 2005, **44**, 539–545.
- 4 X. Z. Zhang, Y. Huang, K. Q. Fu, S. J. Yuan, C. Huang and H. B. Li, *Colloids Surf., A*, 2016, **491**, 29–36.
- 5 M. Cadotte, M. E. Tellier, A. Blanco, E. Fuente, T. G. M. V. D. Ven and J. Paris, *Can. J. Chem. Eng.*, 2007, **85**, 240–248.
- 6 A. Khosravani, A. J. Latibari, S. A. Mirshokraei, M. Rahmaninia and M. M. Nazhad, *BioResources*, 2010, **5**, 939–950.
- 7 Z. P. Song, G. D. Li, F. X. Guan and W. X. Liu, *Polymers*, 2018, **10**, 389.
- 8 A. Blanco, E. Fuente, M. C. Monte, N. Cortés and C. Negro, *Ind. Eng. Chem. Res.*, 2009, **48**, 4826–4836.
- 9 M. H. Lai, P. Liu, H. B. Lin, Y. Q. Luo, H. B. Li, X. Y. Wang and R. C. Sun, *Carbohydr. Polym.*, 2016, **137**, 375–381.
- 10 O. J. Rojas and R. D. Neuman, *Colloids Surf., A*, 1999, **155**, 419–432.
- 11 Y. Huang, X. Z. Zhang, K. Q. Fu, H. B. Li, C. Huang and S. J. Yuan, *J. Ind. Eng. Chem.*, 2015, **31**, 309–316.
- 12 S. B. Buczek, W. G. Cope, R. A. McLaughlin and T. J. Kwak, *Environ. Toxicol. Chem.*, 2017, **36**, 2715–2721.
- 13 X. Xu, Q. B. Han, J. S. Li, L. Liu, M. Li, Y. Z. Du, X. L. Xu, W. Liu, J. H. Wei, P. T. Meng and F. Y. Lu, *China Pulp Pap.*, 2003, **22**, 34–37.
- 14 W. J. Liu, S. B. Wu and Z. Y. Tao, *China Pulp Pap.*, 2013, **32**, 25–30.
- 15 T. S. Renitha, J. Sridevi, M. K. Gowthaman, B. Ramanaiyah and P. Saravanan, *RSC Adv.*, 2015, **5**, 9891–9897.
- 16 G. Y. Li, S. Fukunaga, K. Takenouchi and F. Nakamura, *Int. J. Cosmet. Sci.*, 2005, **27**, 101–106.
- 17 G. J. Piazza and R. A. Garcia, *Bioresour. Technol.*, 2010, **101**, 781–787.
- 18 Q. Liu, Y. D. Shen, G. Q. Fei and J. Mou, *Polym. Mater.: Sci. Eng.*, 2011, **27**, 151–154.
- 19 L. J. Yue, Y. H. You, B. Wang and X. B. Sun, *Environ. Chem.*, 2016, **35**, 1507–1515.
- 20 Y. H. You, X. B. Sun, Q. B. Cui, B. Wang and J. Ma, *BioResources*, 2016, **11**, 6162–6173.
- 21 E. Antunes, F. A. P. Garcia, P. J. T. Ferreira, A. Blanco, C. Negro and M. G. Rasteiro, *Ind. Eng. Chem. Res.*, 2008, **47**, 9370–9375.
- 22 Y. M. Liu, C. Xiao, C. M. Hao, F. R. Tao and J. Y. Li, *Chin. Chem. Lett.*, 2014, **25**, 1193–1197.
- 23 J. A. Deiber, M. L. Ottone, M. V. Piaggio and M. B. Peirotti, *Polymer*, 2009, **50**, 6065–6075.
- 24 M. Bertoldo, F. Cognigni and S. Bronco, *Polymer*, 2012, **53**, 4595–4603.
- 25 Y. H. You, Y. H. Zeng, Y. S. Liu, X. P. Liao and S. Bi, *J. Soc. Leather Technol. Chem.*, 2014, **98**, 69–75.
- 26 W. Z. Zhou, B. Y. Gao, Q. Y. Yue, L. L. Liu and Y. Wang, *Colloids Surf., A*, 2006, **278**, 235–240.
- 27 C. Z. Hu, H. J. Liu and J. H. Qu, *Colloids Surf., A*, 2005, **260**, 109–117.
- 28 B. H. Wortley and J. C. Steelhammer, *MRS Proceedings*, 2011, **197**, 273–278.
- 29 L. F. Ren, X. C. Wang, T. T. Qiang, Y. Q. Ren and J. X. Xu, *J. Soc. Leather Technol. Chem.*, 2009, **104**, 218–226.
- 30 N. N. Fathima, S. Saravanabhavan, J. R. Rao and B. U. Nair, *J. Soc. Leather Technol. Chem.*, 2004, **99**, 73–81.
- 31 W. J. Liu, S. B. Wu and Z. Y. Tao, *Chem. Ind. For. Prod.*, 2014, **34**, 61–65.
- 32 P. G. Dalev, R. D. Patil, J. E. Mark, E. Vassileva and S. Fakirov, *J. Appl. Polym. Sci.*, 2000, **78**, 1341–1347.
- 33 Y. Wang, B. Y. Gao and Q. Y. Yue, *International Conference on Remote Sensing*, 2011, pp. 7267–7270.
- 34 H. J. Liu, J. H. Qu, C. Z. Hu and S. J. Zhang, *Colloids Surf., A*, 2003, **216**, 139–147.
- 35 D. E. Przybyla and J. Chmielewski, *J. Am. Chem. Soc.*, 2008, **130**, 12610–12611.
- 36 W. Hsu, Y. L. Chen and J. C. Horng, *Langmuir*, 2012, **28**, 3194–3199.
- 37 J. Huang, Y. Z. Yuan and H. Liang, *Sci. China, Ser. B: Chem.*, 2002, **45**, 200–207.
- 38 Y. Hu, H. Yu, J. Dong, X. Yang and Y. Liu, *Spectrochim. Acta, Part A*, 2006, **65**, 988–992.
- 39 G. Zhang, A. Wang, T. Jing and J. Guo, *J. Mol. Struct.*, 2008, **891**, 93–97.
- 40 N. P. Camacho, P. West, P. A. Torzilli and R. Mendelsohn, *Biopolymers*, 2001, **62**, 1–8.
- 41 H. Wu, L. Zhuo, Q. He, X. Liao and B. Shi, *Appl. Catal., A*, 2009, **366**, 44–56.
- 42 L. He, H. L. Chen, R. Luo, B. L. Liu and L. Z. Gao, *Macromol. Biosci.*, 2003, **3**, 344–346.
- 43 S. Yang, W. Li, H. Zhong, Y. Wen and Y. Ni, *Sep. Purif. Technol.*, 2019, **209**, 238–245.
- 44 J. Yin, Y. Duan and Z. Shao, *Acta Chim. Sin.*, 2014, **72**, 51–55.
- 45 M. I. Bautista-Toledo, J. Rivera-Utrilla, R. Ocampo-Pérez, F. Carrasco-Marina and M. Sánchez-Polo, *Carbon*, 2014, **73**, 338–350.
- 46 J. L. Guo, X. L. Wang, X. P. Liao, W. H. Zhang and B. Shi, *J. Phys. Chem. C*, 2012, **116**, 8188–8195.
- 47 W. Li, T. Hua and Q. X. Zhou, *Environ. Technol.*, 2011, **32**, 911–920.
- 48 L. Liang, J. K. Tan, Y. L. Peng, W. C. Xia and G. Y. Xie, *J. Colloid Interface Sci.*, 2016, **468**, 358–363.
- 49 T. Tripaththaranan, M. Hubbe, J. A. Heitmann and R. Venditti, *Appita J.*, 2004, **57**, 448–454.
- 50 E. Dickinson and L. Eriksson, *Adv. Colloid Interface Sci.*, 1991, **34**, 1–29.
- 51 S. Forsberg and G. Strom, *J. Pulp Pap. Sci.*, 1994, **20**, 71–76.
- 52 P. Ofori, A. V. Nguyen, B. Firth, C. McNally and M. A. Hampton, *Fuel*, 2012, **97**, 262–268.
- 53 M. Meyer, *BioMedical Engineering OnLine*, 2019, **18**, 24.

